1995

A classification scheme for shale clasts in deep water sandstones

MELISSA JOHANSSON & DORRIK A. V. STOW

Department of Geology, University of Southampton, Highfield, Southampton, SO17 1BJ, UK

Abstract: Shale clasts are widespread in turbidites and associated facies of all ages. They may yield important information regarding the depositional process of the host sandstone and its specific environmental setting. Previous work has tended to generalize the variety of shale clasts that exist and no comprehensive classification has yet been developed. The scheme proposed here is a descriptive classification based on the nature and arrangement of shale clasts within mainly structureless sandstones. Twelve types of clasts are recognized on the basis of the clast's position in the bed and/or characteristic features, and these have been grouped according to whether they have been derived from either basal erosion or disturbance (Group A), flow modification (Group B) or post-depositional disturbance (Group C). These clasts have also been organized into characteristic assemblages which are thought to be indicative of particular depositional environment. The classification scheme when used in association with facies analysis can provide an additional tool for core investigations, contributing to the understanding of permeability barriers and relevant architecture.

Shale clasts are well known from deep-water resedimented successions and have often been described as occurring within thick sandstone turbidites since they were first recognized as such over 40 years ago (e.g. Kuenen & Migliorini 1950; Mutti & Ricci-Lucchi 1972; Walker 1978). During a systematic study of deep-water massive (structureless) sandstones, we have paid particular attention to the presence and nature of shale clasts in a number of field examples around the world. It has become increasingly apparent that previous terminologies within the literature such as 'rip-up clast' (Mutti & Nilsen 1981), and 'floating outsized clasts' (Postma *et al.* 1988) are often used incorrectly and have tended to generalize the wide variety that exists. In fact, shale clasts are highly diverse in their configuration, mode of emplacement and evolution, and therefore warrant a comprehensive classification scheme.

For the purpose of this study, shale clasts are taken as fine-grained (silt–clay grade), coherent sedimentary particles or clasts that occur within a sandstone bed. Compositionally, the clasts may be claystone–mudstone, chalk–micrite or volcaniclastic in nature. The sandstone host beds considered were all deposited in deep-water settings by resedimentation processes. We recognize that similar clasts may also occur in alluvial and pyroclastic deposits and in certain other settings.

The scheme proposed here is a descriptive classification founded on the nature and within bed arrangement of shale clasts. The 12 different clast types can be placed into three categories based on their inferred mode of origin. These include those derived from basal erosion (Group A), erosion and transport (Group B), and post-depositional processes (Group C). Clast types are described by their characteristic features, including average and maximum size, shape, sphericity, position in bed, orientation, lateral extent and density (see below). Their likely method of emplacement is discussed with reference to relevant literature.

It is suggested that correct recognition and classification of shale clasts is important for: (1) better understanding the depositional process of the parent bed; (2) identifying more precisely the depositional setting and proximity to source area; and (3) recognising their potential for influencing wireline log signatures and reservoir permeability.

Classification scheme

The full classification scheme is summarized in Table 1 and described in detail in the following section. The descriptive characteristics used have been developed using the parameters set out below, and are based on the full range of examples studied (Tables 1 and 2).

(1) **Clast size** Where possible an average clast size has been determined for datasets of over 100 individual clasts, according to the Wentworth (1922) grain-size scheme.

From Hartley, A. J. & Prosser, D. J. (eds), 1995, *Characterization of Deep Marine Clastic Systems*, Geological Society Special Publication No. 94, pp. 221–241.

Table 1. *A summary of the characteristic features of the different types of shale clasts*

Type	Average size	Sorting	Shape	Sphericity	Orientation	Position in bed	Lateral extents (m)	Density	Process
A1 Shale clast breccia	Cobble	Very poorly sorted	Very angular	Low sphericity	Random	Whole or base of bed	1–10	High density	Slump debris flow
A2 Scour-lag clasts	Large pebble	Poorly sorted to fairly well sorted	Sub-rounded	Medium sphericity	Transverse to flow	Base of bed	10–20	High density	Traction at base of flow
A3 Rafted clasts	Boulder	Poorly to fairly well sorted	Very angular	Very low sphericity: tabular	Random to sub-parallel	Base of bed	1–10	Low density	Rip-up process
A4 Amalgamation clasts	Small cobble	Fairly poorly sorted	Sub-angular	Low sphericity	Sub-parallel to bedding	Base of bed	10–20	Moderate density	Amalgamation surface
A5 Flame clasts	Small pebbles	Fairly poorly sorted	Sub-angular	Low sphericity	Sub-parallel to bedding	Base of bed	1–10	Low density	Loading and injection
B1 Shale clast conglomerate	Small cobble	Fairly poorly sorted	Sub-rounded	High sphericity	Random	Whole or base of bed	> 20	High density	Cohesive sandy debris flow
B2 Isolated clasts	Cobble	Poorly sorted	Sub-angular to sub-rounded	Low to high sphericity	Random	Anywhere in bed	None	Very low density	Buoyancy
B3 Clustered clasts	Small cobble	Fairly well sorted	Sub-rounded to rounded	High sphericity	Sub-parallel to bedding	Upper mid-bed	> 20	Moderate density	'Floating' on inertia layer
B4 Dispersed clasts	Granule	Well sorted	Sub-rounded	High sphericity	Random/sub-parallel to bedding	Dispersed throughout bed	> 20	Low density	High concentration turbidity current
B5 Lamination clasts	Granule	Well sorted	Rounded	High sphericity	Aligned parallel to lamination/cross-lamination	Base of bed	10–20	Moderate density	Traction at base of flow
C1 Rip-down clasts	Large pebble	Poorly sorted	Very angular	Low sphericity	Sub-paralled to bedding	Top of bed	1–10	Moderate density	Rip-down process
C2 Injection clasts	Granule–cobble	Poorly sorted	Angular	Low sphericity	Random or sub-parallel to the margins of injection	Concentrated near sandstone–shale contact	Localized	High to low density	Ripping process due to sand injection and post-depositional disturbance

(2) **Sorting** This refers to the variation in clast size distribution within any one bed and is described using estimated standard deviations of clast size population (in phi units) as given by Folk & Ward (1957).
(3) **Shape** Shape refers to the degree of roundness or angularity of clasts estimated according to the scheme described by Pettijohn *et al.* (1973).
(4) **Sphericity** Sphericity describes how closely clasts approximate to a sphere, and is divided into low or high sphericity categories (Pettijohn *et al.* 1973). Further qualifying terms such as tabular, elongate, obloid, platy are also given where appropriate.
(5) **Orientation** The orientation of the clasts describes their position (sub-parallel, parallel or random) with relation to bedding features.
(6) **Position in bed** This describes the location of the clasts with reference to the upper and lower boundaries of the bed (e.g. base, middle and top).
(7) **Lateral extent** The lateral extent of the clast zone (where known) has been described as: very extensive, > 20 m; moderately extensive, 10–20 m; little lateral extent, 1–10 m. Isolated clasts or small isolated groups of clasts are described as localized or as having no lateral extent.
(8) **Density** The density or clast concentration within a particular shale clast zone is an estimate of the proportion of core or outcrop surface which comprises shale clasts. The clast area calculated is simply the mean thickness of the clast zone multiplied by a zone length of 100 times the mean long-axis dimension of the clasts. The divisions are as follows: high density, > 60%; moderate density, 30–60%; low density, < 30%.
(9) **Process** The emplacement process for different clast types (as stated briefly in Table 1), is based both on previous work and on interpretation of our own data.

Clast description

Group A

Type A1 – shale clast breccias (Figs 1 & 2). These clasts can vary from pebble to boulder grade (64 to >256 mm) but are generally cobble sized (100 mm). The clasts form very poorly sorted, subangular, matrix-supported, chaotic breccias. These breccias form laterally impersistent zones, orientated subparallel to bedding. The zones occur as shale clast 'nests' between sandstone beds, some of which typically exhibit slump features. In some cases the angular shale clasts can be seen to have been derived from shale beds that have been broken and disrupted by slumping from channel margins.

Type A2 – scour-lag clasts (Figs 1 & 3). These clasts are found in irregular scoured depressions at the basal surface of a bed and are densely packed. The clasts are typically ovoid subrounded, and range in size from small pebbles to large cobbles (> 4 to 256 mm), averaging large pebble size (64 mm). They are poorly to well sorted with random to subparallel orientation and either localized or moderate lateral extent. The zone thickness can vary depending on the depth of the underlying erosive scour and degree of lag deposit development within the host facies. The host sandstone bed may be normally graded with the coarser grain-size fraction forming the shale clast matrix.

Type A3 – rafted clasts (Figs 1 & 4). These clasts can range in size from large pebbles to large boulders (64 to > 256 mm), but are typically boulder sized (> 256 mm). They are found at the base of the host bed and tend to have a low density, occurring singly or in small numbers, with little or no apparent sorting. Clasts are matrix-supported with long-axes tending towards flow-parallel and bed-parallel orientations. They show little evidence of reworking and tend to be tabular in shape, although in some cases partial soft-sediment deformation is apparent. Partially ripped-up clasts also occur still attached to their underlying shale bed. The host sediment tends to have a sharp base with some localized scours.

Type A4 – amalgamation clasts (Figs 1 & 5). These clasts are generally poorly sorted, subangular shaped discs, which range in size from small pebbles to cobbles (> 4 to < 256 mm), but normally average large pebble size (64 mm). The clasts form a matrix-supported layer or zone at the base of the bed often fitting together in a closely knit jigsaw manner to form a competent bed. Sandstones above and below the shale clast zone are typically massive or slightly graded. The clasts can be seen to have been derived from a former shale bed and delineate an amalgamation surface between two sandstone units.

Type A5 – flamed clasts (Figs 1 & 6). These clasts are variable in size ranging from granules to

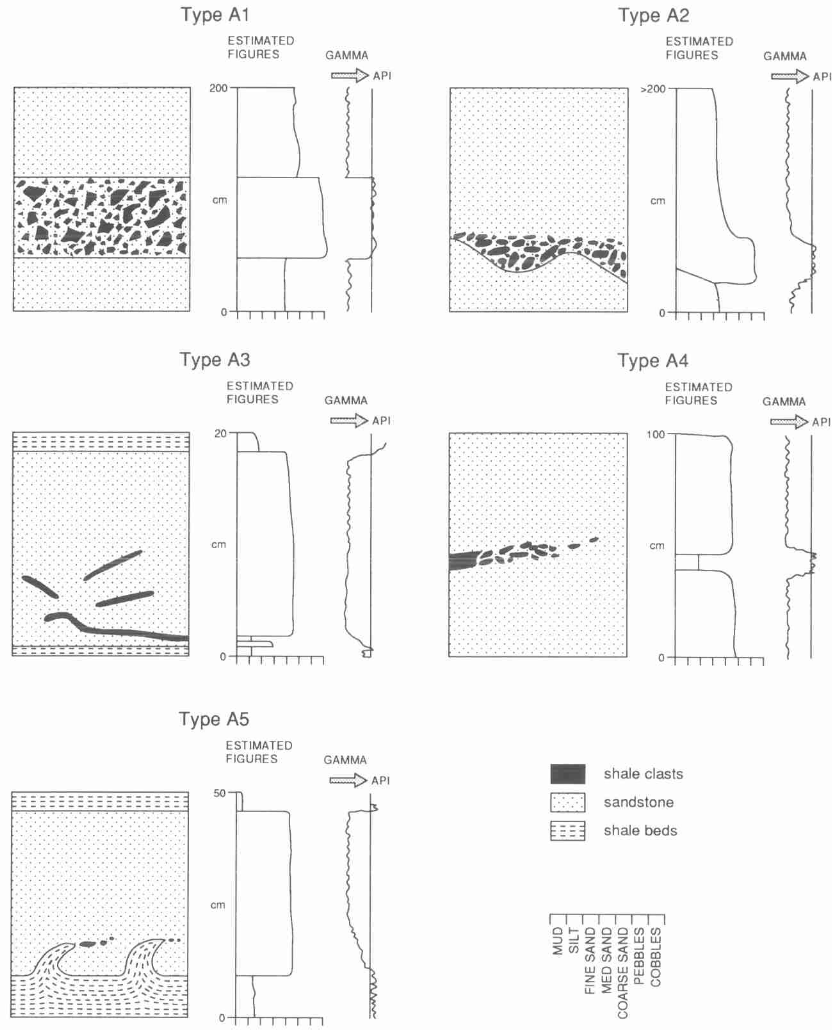

Fig. 1. Group A: clasts formed by erosion disturbance at the base of flow.

very large pebbles (up to 64 mm). They are subangular in shape, often deformed and occur close to their point of detachment from the underlying bed. They are not sorted and have a low density distribution within a matrix-supported sandstone host rock. The host sandstone shows marked loading at its base, which has caused the underlying muddy layer to become over-pressured and squeeze upwards disintegrating in the overlying sandstone.

Group B

Type B1 – shale clast conglomerates (Figs 7 & 8). These conglomerate clasts vary from small pebbles to boulders (4 to > 256 mm) in size, with cobble-sized clasts the most common. They are subrounded, oval-shaped, generally poorly sorted and supported within either a fine sand or muddy matrix. Clasts occur throughout the host bed and clast zones are very laterally extensive. Type B1 clasts differ from Type A1 clasts in being rounded rather than angular in shape. The host bed is generally less chaotic in terms of its internal bedding and lacks slump features. However, some more deformed and angular clasts may also occur with Type B1 clasts, and a complete gradation between shale clast conglomerates and breccias is likely to exist.

Table 2. *Different types of shale clasts found in deep water resedimented sandstone successions*

Host sandstones		
Formation	Locality	Age
Aberystwyth Grits	Dyfyd, West Wales	Upper Llandovery
Albidona	S Italy	Miocene
Andrew Sandstone	Central North Sea (Quad. 30), UK	Palaeocene
Balleny Group	Chalky Island, S New Zealand	Oligocene
Bray Head	Co. Wicklow, Eire	Ordovician
Cabon Conglomerate	Elan Valley, Central Wales	Rhuddianian
Campodarbe (Upper)	S Central Pyreenes, Spain	Middle Eocene
Cantua Sandstone	San Joaquin Valley, California, USA	Early Eocene
Capistrano (Lower)	Dana Point, California, USA	Upper Miocene
Carmelo	Point Lobos, California, USA	Palaeocene
Chatsworth	Los Angeles County, California, USA	Late Cretaceous
Cloridorme	Caspé Peninsular, Quebec, Canada	Ordovician
Conway Castle Grits	Deganwy Quarry, Conway, Wales	Upper Ordovician
Conway Trough	South Island, New Zealand	Neogene
Denbigh Grits	Garn Prys, N Wales	Wenlock, Mid Silurian
Frigg	Norwegian North Sea, Odin Field	Lower Eocene
Gault	Faulknis Nappe, Tschingl, Austenburg	Aptian–Albian
Goldenville	Nova Scotia, Canada	Cambro–Ordovician
Grès d'Annot	Annot, SE France	Lower Oligocene
Grindslow	Ladybowers Res. Pennines, UK	Namurian
Gryphon Sands	Crawford Ridge, northern North Sea	Late Palaeocene–Early Eocene
Habrim Formation	Pohang Basin, SE Korea	Miocene
Hareelv	E Greenland	Upper Jurassic
Heimdal	Sleipner East Field, Norwegian North Sea	Palaeocene
Jackforth (Upper)	DeGray Spillway, Arkansas, USA	Pennsylvannian
Ksiaz	Central Sudetes, SW Poland	Devonian–Carboniferous
Las Vacas	W Argentina	Ordovician (Late Llanvirn)
Loiano Sandstone	Bologna, Apennines, Italy	Middle Eocene
Maesan Fan Delta	Pohang Basin, SE Korea	Miocene
Marnosa Arenacea	Romagna, Apennines, Italy	Early Messinian
Matilija	Santa Ynez Mts, S California, USA	Eocene
Modelo	Los Angeles County, California, USA	Upper Miocene
Mississippi Fan	Louisiana, USA	Upper Pleistocene
Monowai	W Southland, New Zealand	Middle Miocene
Montery Fan	S Central California, USA	Modern
M. Sacro	Campania, S Italy	Upper Miocene
Numidian Flysch	Contrada di Romano, N Sicily	Miocene
Numidian Flysch	Ponte Finale, NE Sicily	Miocene
Otakura	S Otago, New Zealand	Jurassic
Quebrada de las Lajas	E Precodillera Province, Argentina	Carboniferous
Ranzono Sandstone	Emilia, Apennines, Italy	Late Eocene–Middle Oligocene
Reitano Flysch	Cap d'Orlando, NE Sicily	Early Miocene
Rhuddnant/Aberystwyth Grit	Central Wales	Upper Llandovery, Silurian
Rocchetta	NW Italy	Oligocene–Miocene
Sandstone Turbidite (unnamed)	Nizhniye Sergi, W Urals, Russia	Middle Devonian
Shelters Cove	San Francisco Peninsula, California, USA	Upper Cretaceous–Palaeogene
Solitary Channel, Tabernas Basin	Tabernas, SE Spain	Miocene
Sognefjord	Viking Graben, North Sea	Upper Jurassic
S. Mauro, Cliento Unit	Cilento/Campania, Southern Italy	Langhian, Miocene

Clast types											
A1	A2	A3	A4	A5	B1	B2	B3	B4	B5	C1	C2
✓	✓			✓			✓			✓	
✓							✓				
✓						✓	✓	✓			✓
	✓						✓				
								✓			
✓			✓			✓	✓				
					✓		✓				
						✓		✓			
	✓					✓	✓				
✓	✓						✓				
	✓		✓	✓		✓	✓				
					✓						
	✓						✓				
	✓										
						✓	✓				
								✓			
					✓						
					✓		✓	✓			
			✓		✓	✓	✓				
	✓					✓					
											✓
					✓	✓					
			✓				✓				✓
	✓										
✓					✓	✓					
						✓					
	✓						✓		✓		
					✓	✓	✓				
✓						✓	✓				
					✓		✓	✓			
						✓	✓				
		✓	✓								
					✓						
✓	✓			✓		✓	✓	✓			
	✓				✓	✓	✓				
						✓	✓				
						✓					
✓						✓	✓				
						✓	✓				
						✓	✓				
					✓		✓				
					✓			✓			
						✓					
							✓				
	✓										
					✓						
✓		✓	✓	✓		✓	✓	✓			
	✓						✓				
						✓					

Fig. 2. Type A1 – Mudstone Breccia from the Palaeocene, Carmelo Formation, Point Lobos, California, pen for scale (courtesy of B. Cronin).

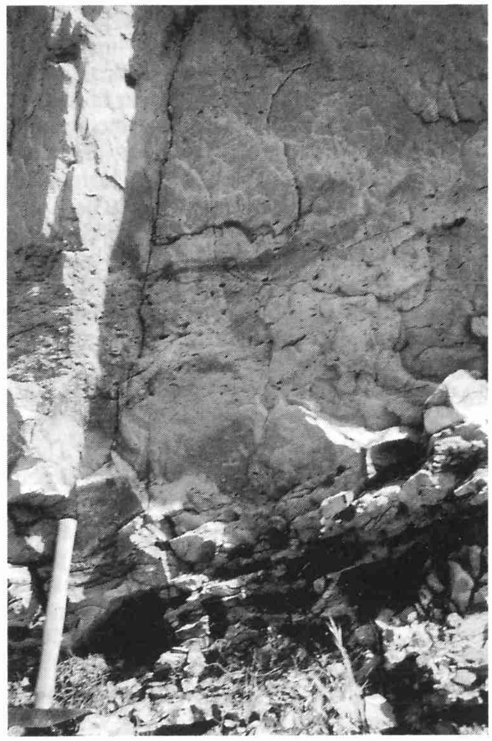

Fig. 3. Type A2 – Scour-Fill Clasts from the Numidian Flysch, Ponte Finale, Sicily, hammer for scale.

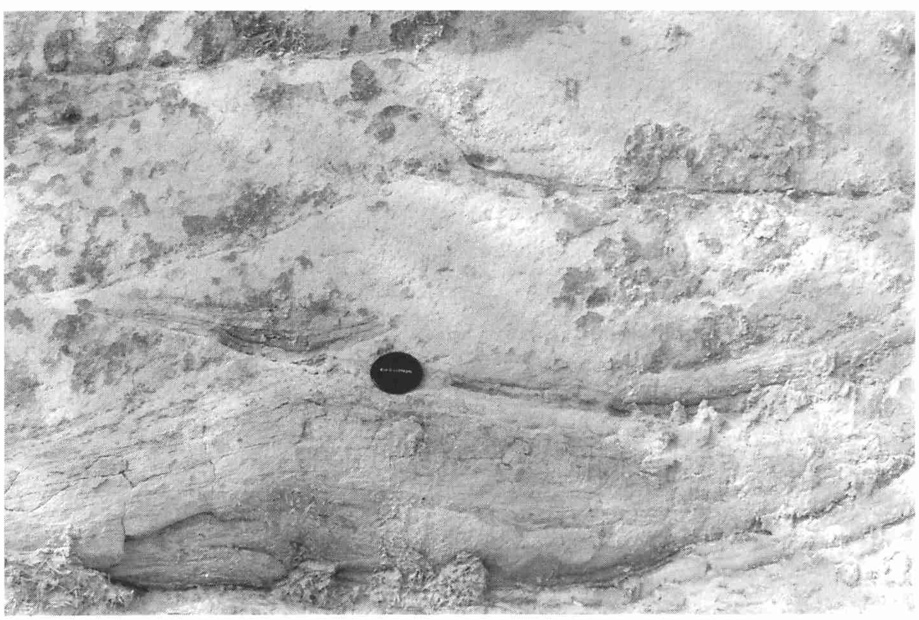

Fig. 4. Type A3 – Rafted-up Clasts from the Oligocene, Grès d'Annot Formation, St Antonin, France, lens cap for scale.

Type B2 – isolated clasts (Figs 7 & 9). These clasts are variable in size, ranging up to and > 5 m in diameter. They are typically subrounded to subangular and ovoid to tabular in shape, with a tendency to become increasingly more tabular with increasing clast diameter. Clasts occur singly or in low density clusters and are of very limited lateral extent. They may occur anywhere within a sandstone bed, but are most commonly found in a lower to mid-bed position, typically along coarse-grained stringers within the host sandstone. Long-axis orientation is parallel to bedding. The host bed generally comprises structureless, ungraded sandstone with a sharp base.

Type B3 – Clustered Clasts (Figs 7 & 10). These clasts are of variable shape and size (small pebbles to large cobbles; 4 to > 256 mm) and are predominantly rounded. They occur in a thin zone along a common plane, orientated parallelto bedding and have a moderate lateral extent. This zone tends to be positioned at a grain-size boundary, normally within an upper mid-bed region. Individual clasts are more randomly orientated within this zone, although with a tendency towards sub-parallel long-axis alignment. The sandstone host beds tend to be structureless and ungraded below the shale clast zone and positively graded above. The basal contact of the sandstone is sharp and can be erosive.

Type B4 – dispersed clasts (Figs 7 & 11). This type of clast is characterized by its small size (2–4 mm), rounded to subrounded nature and equant to ovoid shape. However, dispersed clasts up to 20 cm in diameter have also been observed. Clasts are typically size sorted (i.e. positively graded) throughout the bed, with bed-parallel orientation. Although in most cases the clasts form the coarse-tail of a normally graded bed, dispersed clasts have also been observed in reverse-graded and ungraded sandstones.

Type B5 – lamination clasts (Figs 7 & 12). These clasts are, on average, granule sized (2–4 mm), well sorted, well rounded and of a high sphericity. Clasts tend to be associated with the coarse fraction of the host sandstone and may be aligned along any primary sedimentary structure (e.g. cross- or parallel-lamination).

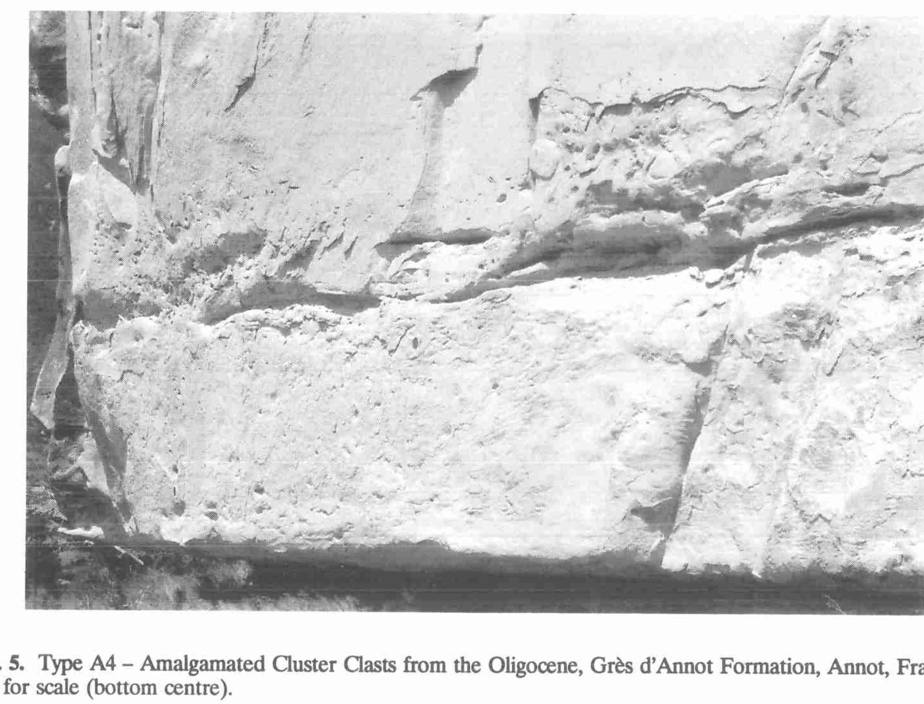

Fig. 5. Type A4 – Amalgamated Cluster Clasts from the Oligocene, Grès d'Annot Formation, Annot, France, hat for scale (bottom centre).

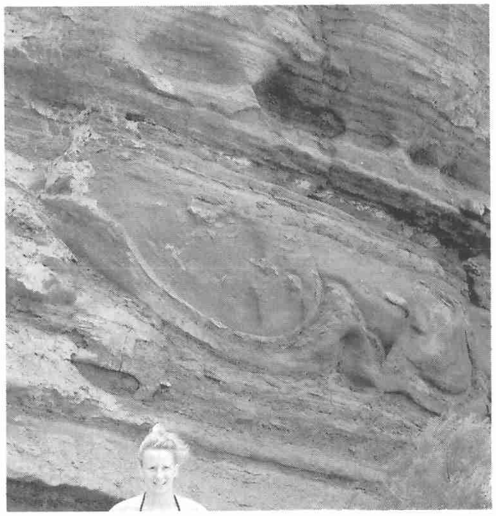

Fig. 6. Type A5 – Flamed-Up Clasts from the Miocene, Muddy System, Tabernas, Spain, person for scale.

Group C

Type C1 – rip-down clasts (Figs 13 & 14). This clast type is characteristically small in size, generally no larger than small cobbles (100 mm). Clasts are extremely angular, with very low sphericity and are often sheared resulting in a contorted or wavy appearance. They are generally poorly sorted and commonly show a weak preferred orientation parallel to bedding. The only visible organization is a crude reverse-grading observed within some beds, with the larger clasts in close association with the upper boundary whereas smaller clasts are positioned lower within the bed. The density of these clasts tends to decrease downwards, although the actual number of clasts may increase. In some cases, clasts occur still partly attached to the upper boundary surface and extend into the underlying sandstone bed.

Type C2 – injection clasts (Figs 13 & 15). These clasts range in size from small pebbles to medium cobbles (4–200 mm). They are extremely angular and often strongly deformed. They can occur anywhere within the host sandstone, singly, dispersed or in distinct zones. They can be distinguished from A4, B2 or B3 clast types by their angularity and sheared (deformed) nature and by the discordant boundary contacts of the host sandstone.

Inferred processes and examples

The characteristic features and distinguishing qualities of the different types of shale clast are summarized in Table 1, with the most distinctive of these parameters being size, shape, sphericity and within-bed position. It is thought that the principal control on these parameters is the origin of the clasts and their subsequent modification by flow processes. Clasts, can therefore be subdivided into three categories depending on whether they have formed from base of flow erosion, flow modification or through post-depositional erosion.

Group A: base of flow erosion or disturbance

Group A comprises shale clast types derived from erosion or disruption of the underlying or laterally adjacent beds during the flow that deposited the host sandstone.

Type A1 – shale clast breccia. These clasts form from the total disruption and dislocation of a shale bed or beds due to slumping. When a composite unit of semi-consolidated interbedded shale and sandstone is involved in slump folding, there is a tendency for the more competent mud beds to fracture whereas sandstones are more likely to undergo liquefaction. Therefore, the mud material forms fragmented clasts within a disaggregated sand matrix. Where such slumping and bed disruption occurs independently of turbidity current flow within the channel (e.g. by channel-margin collapse), then transport distance is unlikely to be great, and a lenticular bed or nest of shale-clast breccia will be deposited close to the zone of slumping. Subsequent down-channel flows may partially winnow and erode the irregular mound causing some rounding of clasts at the surface. Similar clasts have been described by Rupke (1976) and Johns *et al.* (1981) from the Roncal Unit in the Eocene Turbidites of the southwestern Pyrennees. Channel margin slumping initiated by and coincident with turbidity current flow within the channel will subject any shale clasts formed to a greater degree of abrasion and potential incorporation into the flow. This can then give rise to Type A2 and various Type B clasts.

Type A2 – scour-fill clasts. These clasts are thought to be mainly derived from basal plucking of the channel floor by a highly competent turbidity current. They are then transported in a base-of-flow high-concentration inertia layer or

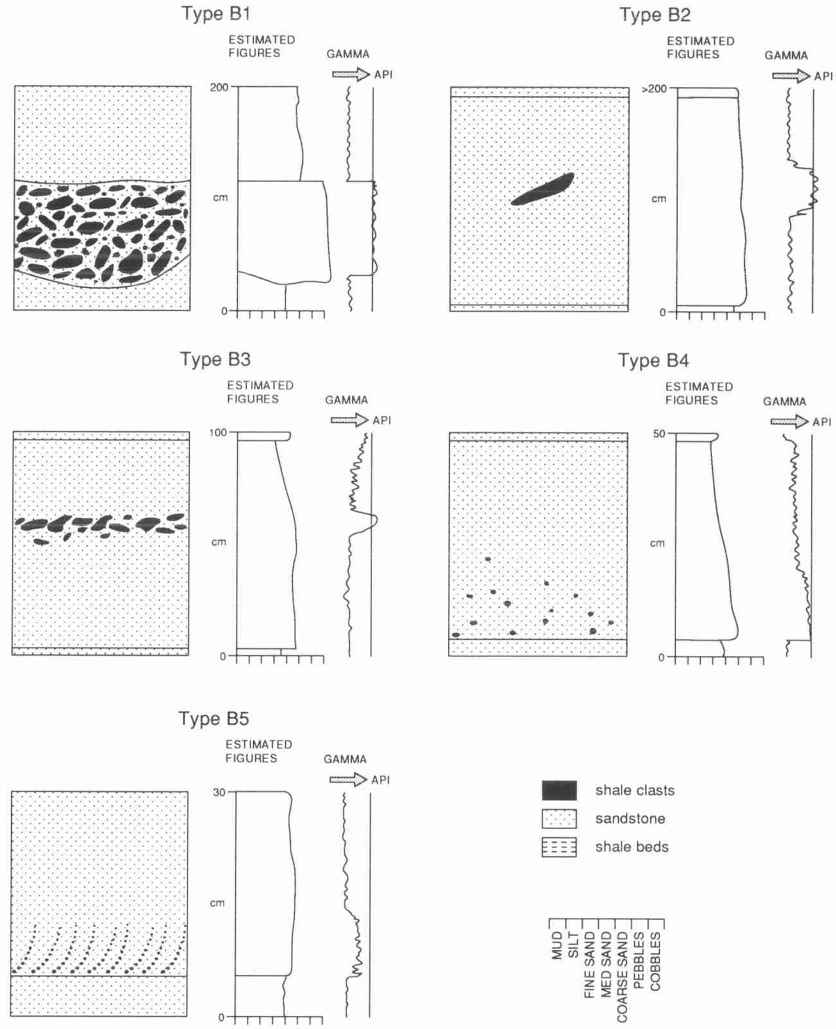

Fig. 7. Group B: clasts modified during within flow transport.

traction carpet, and are not incorporated into the overlying fully turbulent part of the flow. Transport distance is very limited and flow modification slight so they are not classified with our fully flow-modified Type B clasts. Clasts concentrate at the base of thick, channelized sandstone beds and represent the cessation of rolling, saltation or gliding of the shale clast bedload in such high concentration flows. Deposition commonly occurs in deep erosive scours. Type A2 clasts may also form by channel margin slumping and bed disruption coincident with turbidity current flow. Examples of these clasts have been described by Chipping (1972) from Cretaceous and Palaeocene sandstones at Shelters Cove and Devils Slide on the San Francisco Peninsula.

Type A3 – rafted-up clasts. As with the scour-fill clasts, rafted clasts form from erosion at the base of a highly competent sand-laden turbidity current. However, in order to form rafted-up shale 'flaps' that are still partly attached to the underlying bed, the current must erode the shale bed and deposit its load almost simultaneously. Other clasts may become completely detached from the substrate or broken from a larger slab, but are frozen in the depositing flow before being transported any great distance. Their point of origin can often be seen as a tabular erosive scour in the underlying shale. Clasts of this type are well known from many deep-water sandstone formations worldwide [e.g. Modelo Formation, Los Angeles (Sullwold 1960); Solitary Channel, SE

Fig. 8. Type B1 – Mudstone Conglomerate Clasts from the Miocene, Muddy System, Spain, lens cap for scale.

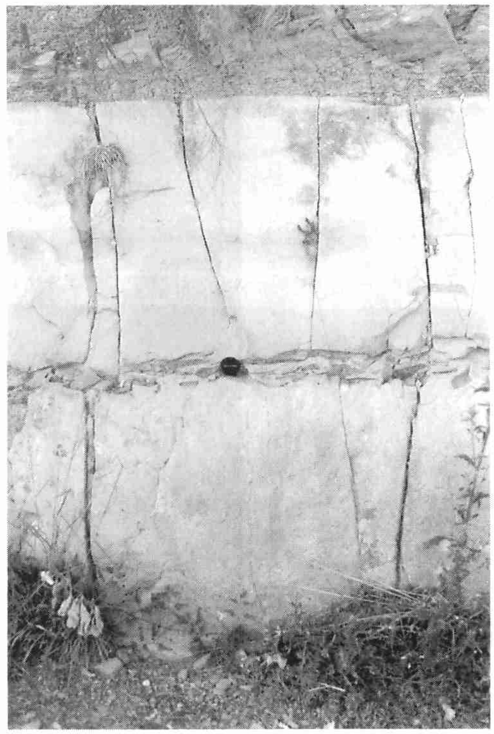

Fig. 10. Type B3 – Cluster Clasts from the Oligocene, Grès d'Annot Formation, Piera Cava, France, lens cap for scale.

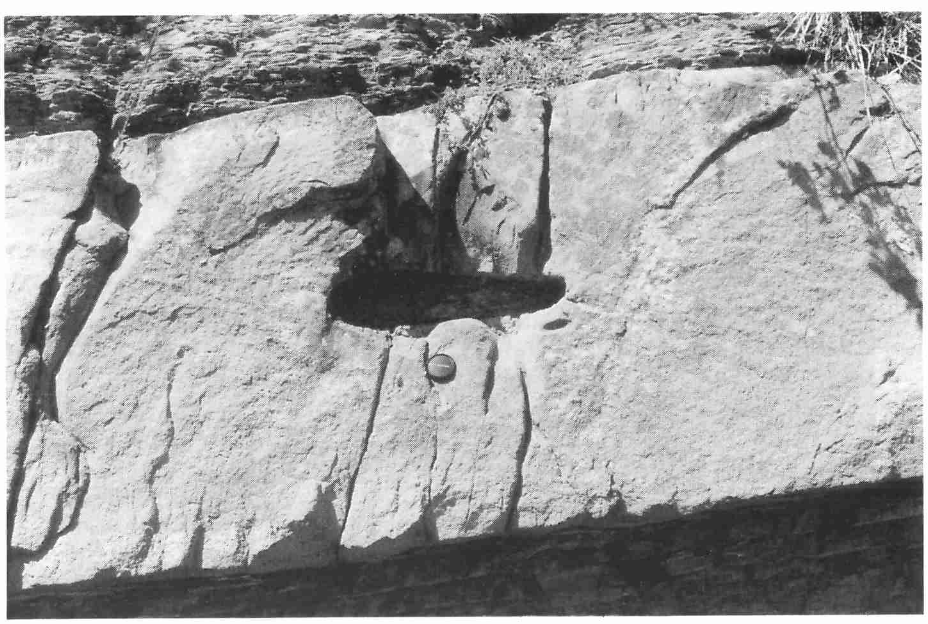

Fig. 9. Type B2 – Isolated Clasts from the Oligocene, Grès d'Annot Formation, Piera Cava, France, lens cap for scale.

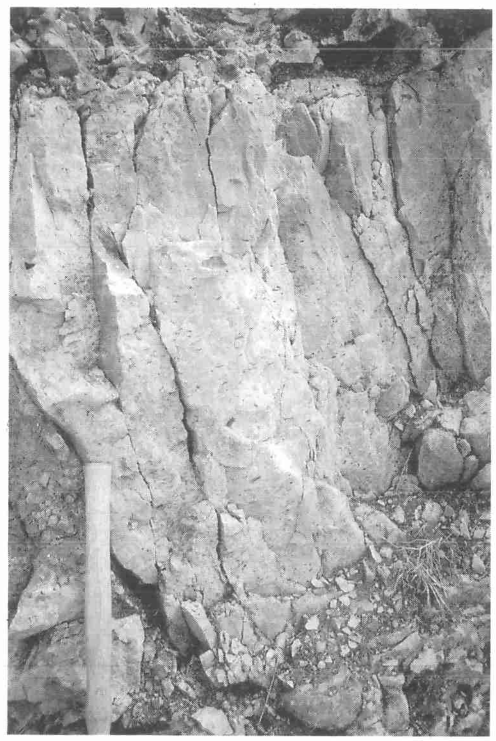

Fig. 11. Type B4 – Dispersed Clasts from the Numidian Flysch, Ponte Finale, Sicily, Hammer for scale.

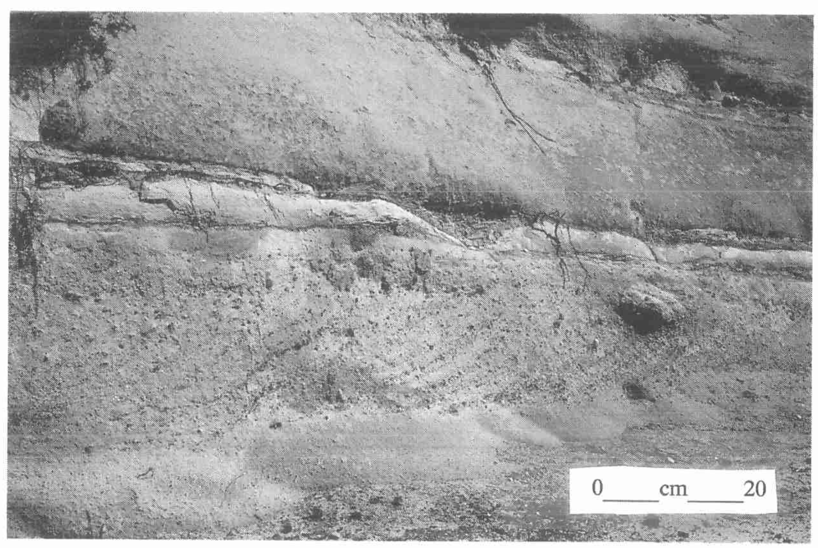

Fig. 12. Type B5 – Lamination Clasts in the form of cross sets from the Oligocene, Grès d'Annot Formation, St Antonin, France, bar for scale.

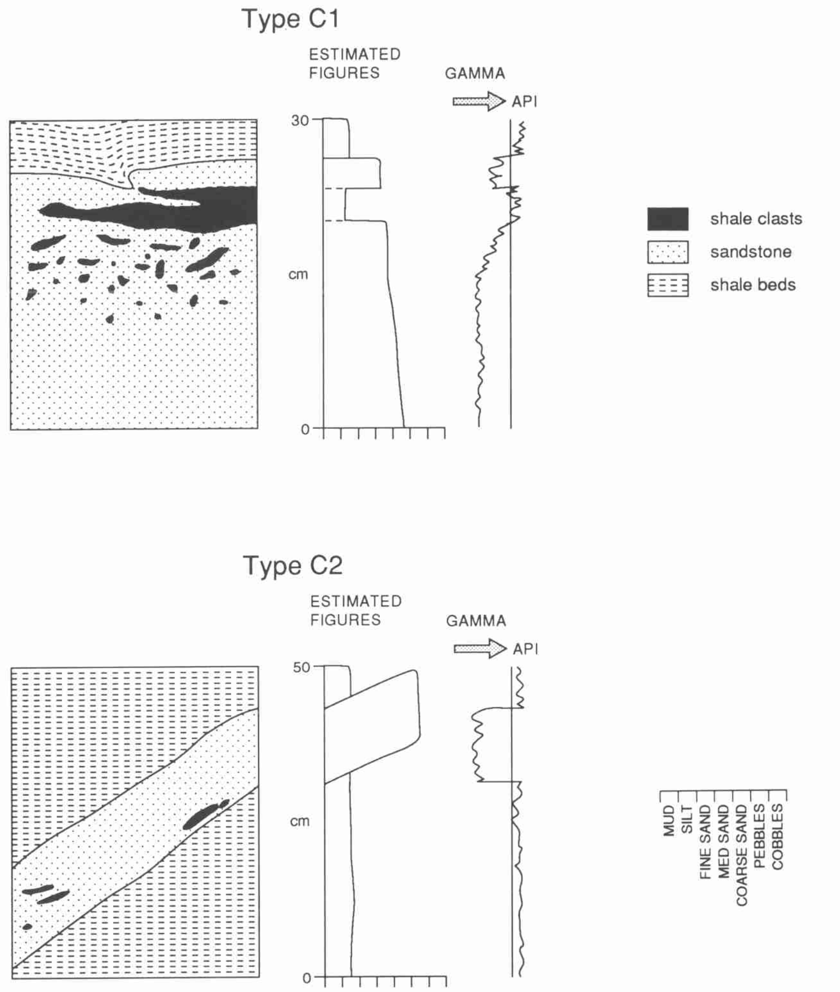

Fig. 13. Group C: clasts formed by post-depositional erosion.

Spain (Kleverlaan 1989)]. They are also known as 'rip-up' clasts.

Type A4 – amalgamation clasts. In general, Type A4 clasts are the product of either: (1) loading by a newly deposited or depositing sandstone unit into and through an intervening semi-consolidated shale bed which overlies a previously deposited sandstone bed; or (2) through the erosive scouring and break-up of a thin shale bed. The chief requirement is that the shale bed is sufficiently competent or brittle to break up into clasts when loaded or eroded. Clasts remain at the base of the flow and are deposited more or less *in situ* along the erosive-loaded contact between the two sandstone units. The distinction between A4 and B3 clasts is that the former can be traced laterally into an undeformed, unbroken shale bed between sandstones, whereas the latter are no longer attached to their parent bed. Examples of amalgamated clasts are seen in the Cretaceous Chatsworth Sands, Southern California in the Simi Hills (Link *et al.* 1981).

Type A5 – flame clasts. These clasts originate from flame structures developed by intense loading of a sandstone into an underlying shale bed. They can be recognized as small isolated clasts associated with the lower bed. Their development is due to the inherent instabilities of sand depositing rapidly on to a soft or semi-consolidated muddy substrate. Experimental work has demonstrated that deformation of an underlying silt and mud layer leads to intrusions into an

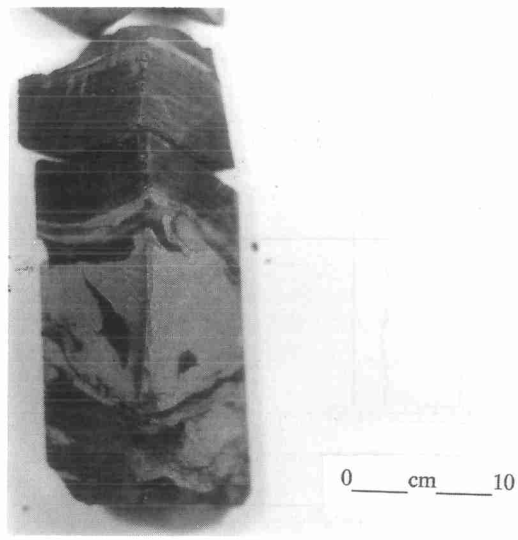

Fig. 14. Type C1 – Rip-Down Clasts from the Volgian Humber Group (Upper Jurrasic), South Viking Graben, North Sea.

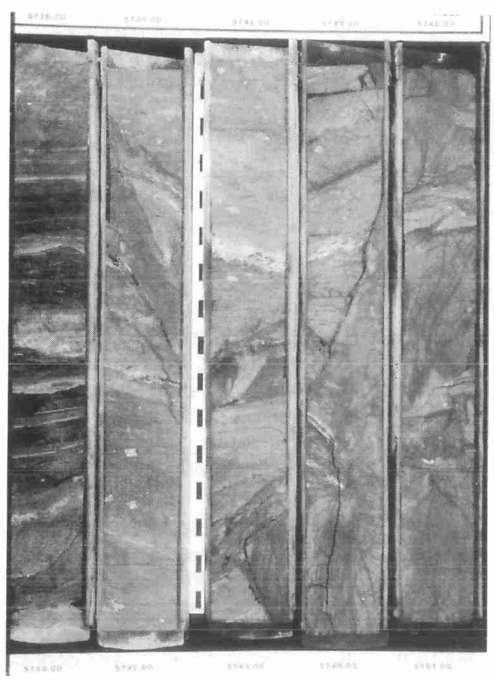

Fig. 15. Type C2 – Sand-Ripped Mud Clasts from Palaeocene Cores from the Central North Sea (Courtesy of J. Reynolds).

upper sandy bed (McKee & Goldberg 1969). This is mainly due to the sudden deposition of overburden on a highly mobile substrate (Kuenen & Menard 1952; Anketell *et al.* 1970). Further movement of the still mobile depositing sand causes some of the projecting flames to break-up and become incorporated into the lower unit of the depositing sand bed.

Group B: clasts modified by transport within-flow

Flow-modified shale clasts are first incorporated into the flow as a result of processes such as erosion of the channel floor and walls, slumping or sliding of the channel margin or head region, or free fall of rocks and shale blocks from steep slopes. The clasts are thus derived from semi-consolidated sediment at the channel margin, head region or from an underlying substratum. During the flow of a turbidity current, large shear stresses can cause the upward movement of an eroded shale clast (Kano & Takeuchi 1989). During transportation, eroded particles are subjected to dynamic forces within the current. Comparatively large grains, especially when travelling close to the static bed, can be influenced by hydrodynamic lift forces arising from the restriction placed on the motion of the fluid by the proximity of the bed. A particle in relative motion within a sheared fluid moves along the gradient of relative velocity and across the line of flow (Allen 1982 85–88). In most cases these shale clasts become incorporated within the basal denser portion of a sand-rich turbidity current or sandy debris flow. Within this flow the semi-consolidated clasts begin to disintegrate due to clast–clast and clast–matrix interaction. The extent to which a shale clast can tolerate the abrasive qualities of the flow interior is as yet unknown, although it is assumed that the clasts would have a relatively short life span. The 'soft' intraclasts survive either through a process of contemporaneous erosion/influx, minimum transport and rapid deposition, or through rapid transformation in the flow behaviour during transport. It is thought that the increased energy expenditure at the base of the flow during transport of large clasts and the incorporation of the increasing fine fraction could possibly suppress the turbulence within the flow resulting in better clast preservation potential (Postma *et al.* 1988).

Type B1 - shale clast conglomerates. These conglomerates are interpreted as sandy debrites in which the shale clasts are intraformational, most likely derived from slumping or erosion. The clasts are transported by a matrix-supported cohesionless sandy debris flow which may occur in isolation or at the base of a turbidity current. Alternatively (or in addition), the sandy debris flow may be driven by the overriding turbidity current. An example of this clast type has been described by Tanaka *et al.* (1992) from the Chrystalls Beach Complex, Caples Terrane, New Zealand.

Type B2 – isolated clasts and Type B3 – clustered clasts. It is the occurrence of both single isolated shale clasts and small groups or clusters of clasts apparently suspended in a mid-bed position that has proved the most difficult to explain and caused much speculation. Several of the proposed mechanisms described below are valid, and each may apply to different examples observed in the field.

(1) One possible mechanism of formation is that the shale clasts are influxed into the flow and emplaced through the gradual aggradation of sediment (Kneller 1995). The transporting current is a sustained steady or near-steady flow, involving a flow boundary that is dominated by hindered settling. Deposition is thought to continue as long as the downward grain flux to the deposit is balanced by sediment supply from the transport regime. The high downward grain flux generates a dense, non-turbulent zone dominated by hindered settling at the base of the flow, with no sharp interface at the depositing surface and no traction. Deposition occurs incrementally from the base (gradual aggradation of Branney & Kokelaar 1992), and is maintained for as long as the flow continues to provide sediment to the zone. As the sedimentation of the sands need no longer be instantaneous but instead gradational, the outsized clasts that occur mid-bed may always have been close to the depositing surface and are pushed up during incremental deposition. It is thought, therefore, that the clasts would have no visible grain-size boundary above or below them and that their locality is determined by the position within the steady flow of the shale clast influx.

(2) Results from flume experiments suggest that mid-bed shale clasts may settle through a flow and alight on an already developed high density inertia-flow layer (Postma *et al.* 1988). This high density flow layer displays pseudolaminar behaviour due to the suppressed turbulence caused by a high particle concentration (Bagnold 1954; Lowe 1982). The large outsized particles then 'glide' along the top of the underlying pseudolaminar inertia-flow layer. The particles become partly submerged within the inertia-flow layer and are driven by the downflow component of turbulent shear–stress transmitted from the overlying, faster moving turbulent layer. As the inertia-flow layer freezes and a new one forms or as the layer thickens, the gliding clasts may be forced to a progressively higher level within the flow. When the deposit eventually ceases to flow the clasts are prevented from returning to the base due to the underlying sediment and are isolated within the bed. It is thought that the uppermost clast formed in this kind of fluid regime would delineate an interface between a grain-size boundary, with the lower sand being massive with possible tractional evidence, and the upper sand exhibiting positive gradation.

(3) In some cases, shale clasts are ripped-up and become fully incorporated into the basal, denser portion of a sand-rich turbidity current (Mutti & Nilsen 1981). Density differences between the lower density, fluid-saturated clasts and the higher density basal sandy layer of the flow would allow the clasts to float upwards through the basal layer. The buoyant upward movement of clasts within the dense basal portion of the current is accompanied by their progressive disaggregation and erosion. Clasts that are not completely dissagregated accumulate in an apparently aligned zone (i.e. clustered clasts, Type B3). This specific position within the bed is thought to be the boundary between the graded Bouma Tb division and the current laminated Bouma Tc division. This division is thought to correspond to the separation between high and low density flow conditions within the current although field evidence suggests that the clasts lie predominantly between the Bouma Ta and Tb divisions.

(4) Early theories suggested that mid-bed shale clasts were typical of grain-flow deposits (Stauffer 1967), with the mid-bed position attributed to kinetic sieving as a result of dispersive pressures (Bagnold 1954, Jullien & Meakin 1992). However, according to Bagnold (1956), the magnitude of dispersive stress is directly dependent on the grain size of the shearing sediment flow and hence would be relatively low in a sandy grain flow (discussion by Middleton & Southard 1978). This mechanism could, therefore, only account for relatively small shale clasts in coarse sandstones, provided that the grain flow can travel far enough after incorporation of the clast(s) for the process to operate (Lowe 1982).

Type B4 – dispersed clasts. These clasts occur in thick normal and reverse, coarse-tail graded beds, as well as in apparently ungraded units. Normal coarse-tail grading occurs where the size of the coarsest grains decreases upwards within a bed, whilst the size of the host grains remains constant. This grading implies turbulence and effective grain interaction during transport, whereas ungraded beds usually indicate high shear strength or high viscosity, thereby preventing the turbulence and effective grain interaction. The coarse-tail inverse grading probably develops from larger clasts rising upwards due to dispersive pressures or by progressive loss of larger clasts, from the lower, more strongly sheared part of the flow (Allen 1982). This type of clast is present in the Numidian flysh 'externe', Sicily (Braakenburg 1994).

Type B5 – lamination clasts. These shale clasts are small in size and closely associated with the coarser fraction of the sandstone bed. They are considered to have behaved as normal particles within the flow, hydrodynamically equivalent to the coarse sands with which they occur. Those clasts deposited along the foresets of large-scale cross-strata have undergone a period of tractional movement and downcurrent bedform migration immediately prior to deposition.

Group C: clasts formed by post-depositional erosion

Some types of shale clast are derived from post-depositional disturbance of a sandstone unit. In this case a semi-unconsolidated sand is remobilized after burial through dewatering and liquefaction caused by sudden shock, natural slope instability and slumping, or simple overburden pressure. The sand flow or injection that results is thought to be pressurized and cohesive, with an ability to erode or pluck shale clasts from either margin of the flow but with a limited transport potential. The clasts are thus largely unreworked but many exhibit some shearing. The processes generating them can include either the 'ripping-down' of an overlying shale bed (Type C1) or the breaking-up of an interbedded shale bed through sand injection (Type C2). In both cases, angularity and partially attached shale clasts help confirm the origin of those that have become fully detached.

Type C1 – rip-down clasts. These clasts were first described as 'rip-down' clasts by Chough & Chun (1988), who suggested that shearing and fragmentation of an upper shale bed in the late Cretaceous Uhangri Formation was caused by penecontemporanous deformation and liquefaction related to intrastratal flow of the lower bed. In this situation, once a sandstone underlying a shale bed is liquified, it may creep and flow within the strata moving either downslope or down-pressure gradient, and may rip-down parts of the overlying layer (Chough & Chun 1988). The downward movement of clasts within the intrastratal flow may result in the break-up of larger clasts potentially resulting in apparently reverse graded zones. Liquefaction can be enhanced by an impermeable cover, such as an overlying shale bed, raising the pore-water pressures and diminishing the effective stress (Finn *et al.* 1977; Allen 1982).

Type C2 – injection clasts. Burial of thick, massive sandbodies, isolated within mudstones, creates a large potential for injection as sand dykes or sills into the surrounding sediment due to overpressuring of pore waters. Sands are thought to be injected in a fluid state, being mobilized by liquefaction during dewatering (Surlyk 1987; Dixon *et al.* 1995). Clasts are formed through a ripping process resulting from the high fluid pressures of the sand during injection into the surrounding substrate. This clast type has been described from the Upper Jurassic Harleev Formation of East Greenland (Surlyk 1987) and the Tertiary of the North Sea (Dixon *et al.* 1995).

Discussion

Classification scheme

The classification scheme proposed here has concentrated entirely on shale clasts in deep-water successions and has further focused on generally thick-bedded sandstone facies in which shale clasts are particularly common. Micro-shale clasts occur in fine-grained turbidite successions, for example in silt laminae at the base of graded-laminated units (Cremer & Stow 1986, Piper & Stow 1984), and in contourite facies (Mézerais *et al.* 1993). The types and processes of origin are most likely analogous to those we have described for their coarser-grained counterparts. Furthermore, shale clasts are a common component of many deep-water conglomerates, in which their origin and behaviour is exactly the same as for the other pebble components of coarse-grained resedimented deposits (Pickering *et al.* 1989).

The 12 clast types defined here are believed to be a good representation of the diversity of clasts which exists. However, it is by no means always possible to classify any particular shale clast with certainty if its full context is not known. This is especially true of shale clasts recognized in cores recovered from hydrocarbon reservoirs/prospects. The characteristic features given in Table 1 are designed to help with clast identification and hence with interpretation.

Clast Origin

Type A clasts. These are formed by erosive processes including disruption of slumps and slides, rock-fall and bank collapse, the rip-up of underlying beds, the break-up of thin intercalated shales, and the flame-up of soft shales due to loading. Although these processes are understood in general terms, the precise cause and mechanism of base-of-flow erosion and break-up is still not fully understood. It seems likely that a gradation in erosive power of the flow, from greater to lesser, gives rise to scour-lag, raft, amalgamation and flame clasts in that order (i.e. A2, A3, A4, A5). This same order could indicate something about the relative erodibility of the substrate which may, in turn, be influenced by the timescale between flow events.

Type B clasts. Those are clasts that have undergone further modification during transport. Shale clast conglomerates (B1) are best interpreted as sandy debris flows. The relatively common occurrence of these clasts in ancient successions indicates that this process is common. Dispersed clasts (B4) and lamination clasts (B5) are those that have become fully integrated into a flow, following extensive break-up and abrasion, and hence behave as the normal coarse fraction of that flow.

The isolated and clustered clasts (B2 and B3) lie somewhere in between the others in terms of origin. Their specific characteristics and context can give information about the nature of the high energy resedimentation event that was responsible for their emplacement. In most cases their presence supports the concept of a bipartite flow, in which the shale clasts were deposited at the interface of an underlying higher-concentration zone and an overriding lower concentration turbulent flow. Where the basal layer was an inertia flow followed by rapid freezing and deposition, then the underlying sandstone will be massive or show some tractional features and the overlying sandstone will typically be graded. Where there was a basal zone of hindered settling and gradual aggradation from a near-steady flow, then the whole unit may appear massive with no change in grain size or structure across the shale clast zone. Smaller and less dense shale clasts may float upwards through a depositing turbidity current and come to rest between the Bouma Ta and Tb divisions. Each of these slightly different characteristics has been observed in the rock record, so that the inferred flow processes are all likely to occur.

Proximal to distal variation

The types and abundance of shale clasts that occur can be used to infer relative proximality in a deep water setting. More proximal settings with slide scars, canyons and gullies are characterized by relatively large numbers of erosive Type A clasts as well as shale clast conglomerates (B1). Medial settings with channel–levee complexes and interchannel areas are characterized by both Type A and Type B clasts that have been modified by transport. In distal distributary channel–lobe settings, Type B clasts dominate, and most of these do not make it out into the most distal basin plain settings. These are characterized by B4 dispersed clasts, B5 lamination clasts and by microshale clasts in fine-grained turbidites.

The same broad trend is evident within well-established channel systems from their margins towards their axis, although with greater variability. Clasts associated with channel margins tend to be shale clast breccias and scour-lag clasts (A1 and A2), and these pass transitionally into A3 raft clasts, A4 amalgamation clasts and Type B clasts. In coarse, gravel-filled channel thalwegs, few clasts are preserved due to very high energy levels, but remnant shale clast breccias (A1), shale clast conglomerate debrites (B1) and scour-lag clasts (A2) may be present. Immediately adjacent to the channel on the proximal levees, thin sandstones may be characterized by intensely disturbed and balled structures with A5 flame clasts.

Depositional environment

Based on detailed observations of some 12 field examples in which thick structureless sandstone units occur in association with a wide variety of more normal turbidite–hemipelagite facies, we can be even more specific in characterizing specific parts of the deep water environment by their shale clast content and type (Fig. 16). The sedimentary environments in which these deep water sandstones occur with their various shale clast types include: fan-delta (plus coarse-grained slope-apron), muddy slope-apron, fan channel–

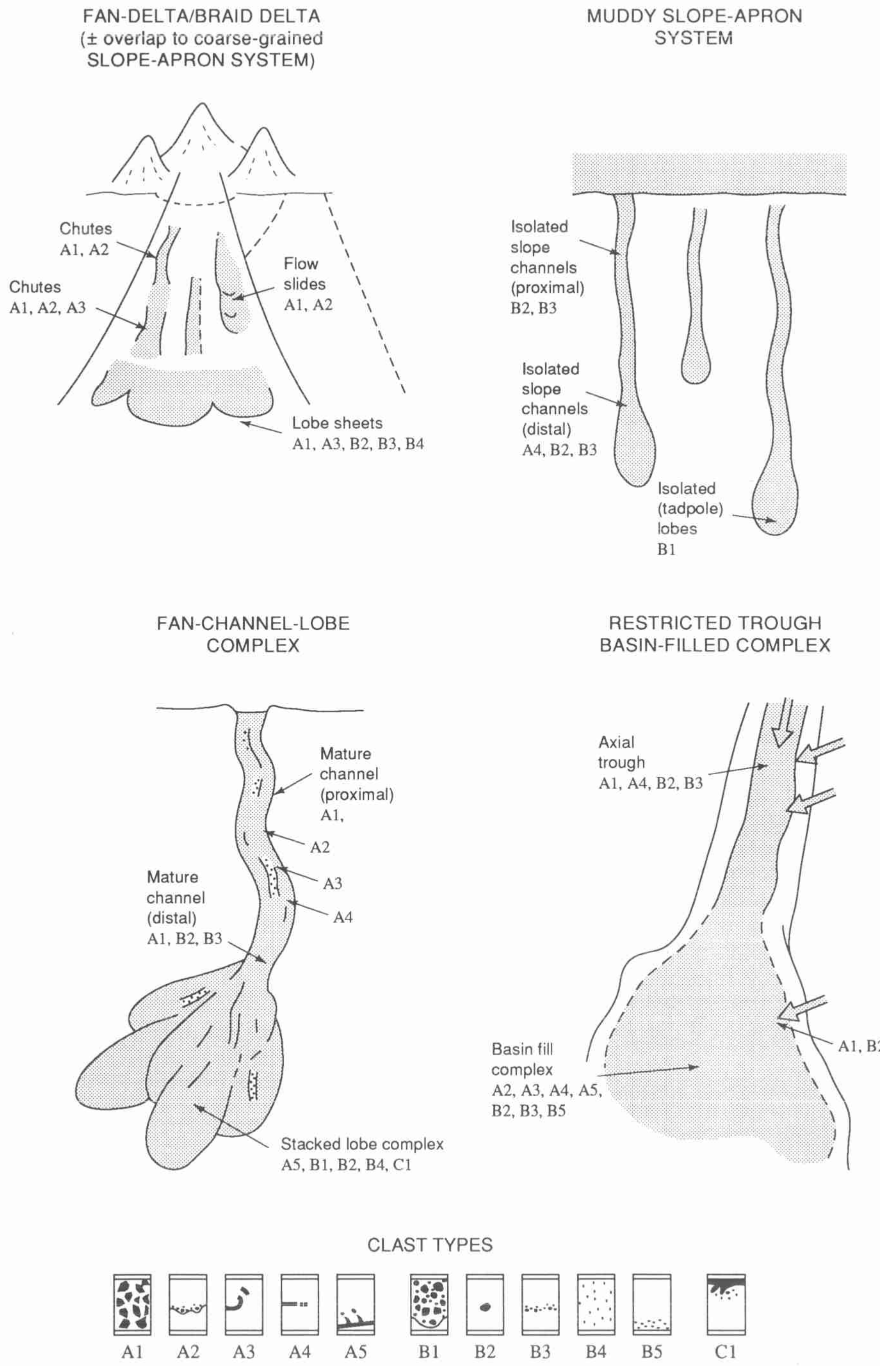

Fig. 16. Model for shale clast distribution within various deep marine environments.

lobe complex and restricted trough–basin-fill complex.

Fan Deltas. These develop where an alluvial fan or braided channel feeds directly on to a subaqueous slope margin. Overlapping fan deltas coalesce to form a coarse-grained slope-apron system. The main processes and features related to this type of environment are chutes, channels, flow slides and lobe sheets. Fan delta chutes and channels are both characterized by A1 mudstone clast breccias and A2 scour-fill clasts. The former clasts are derived from channel-margin collapse and the latter from tractional flow. The channels can be distinguished from the chutes by the presence of an additional clast type, the A3 rafted-up clast. Flow slides are formed by sediment gravity collapse and can be recognized by A1 shale clast breccias and A2 scour-fill clasts. The A2 clasts are thought to be carried as a tractional basal lag. The fan delta lobe sheets are mixed-grade depositional bodies that can be characterized by four types of clast: base-of-bed A4 amalgamated clasts and flow modified B2 isolated clasts, B3 clustered clasts and B4 dispersed clasts. Although there is still some erosion of the underlying shale beds, the majority of clasts are of a depositional nature and are probably derived from previous up-fan erosion.

Muddy slope-apron systems. These are linearly sourced from the platform with mainly fine-grained sediment. The sands form immature channels and lobes which have a tadpole morphology. The proximal isolated slope channels typically contain either B2 isolated or B3 clustered clasts, probably derived from rock-fall or bank collapse. The more distal isolated slope channels have A4 amalgamation clasts as well as B2 and B3 clasts. This is probably due to a slightly lower energy level than the up-channel system. The isolated (tadpole) lobes, however, tend to have B1 debris-flow clasts which have passed through the channel and have deposited due to a reduced carrying capacity within the lobe.

Fan channel–lobe complex. This comprises a high energy, confined, mature channel that feeds into an unconfined, stacked lobe complex. The channel system may contain any of the erosive A-type clasts, with A1–A5 down-channel and across-channel variation in clast types. B1 shale clast conglomerates, B2 isolated clasts and B3 clustered clasts are also common in channels, together being indicative of high energy flows, slumping and tractional processes. The stacked lobe complex is a more variable system with flows switching position on the lobe surface. The environment is predominantly a depositional one, with the main erosional clast forming due to rapid deposition (A5 flame-type clasts). The flow-modified clasts include B1 mudstone clast conglomerates, B2 isolated clasts and B4 dispersed clasts.

Restricted trough–basin-fill complex. This refers to a tectonically confined narrow trough and/or restricted basin which may be variously fed by fan deltas, slope gullies or channel complexes. It can been divided into four subenvironments: the axial trough, basin-fill margin, proximal basin-fill and distal basin-fill complex. The axial trough is characterized by A1 mudstone clast breccias and A4 amalgamated clasts derived from basal erosion, together with B1 mudstone clast conglomerate, B2 isolated clasts and B3 clustered clasts. The basin margin may show a variety of Type A erosive clasts, in particular, A1 chaotic clasts and B2 isolated clasts. The proximal basin-fill complex is close to the mouth of the axial trough and forms a transition between erosion and deposition. The facies have four predominant types of shale clasts, low energy A3 raft-type clasts and A5 flame-type clasts, and flow-modified B3 clustered clasts and B4 dispersed clasts. The more distal basin-fill complex typically displays a greater variety of clast types. The erosive clasts tend to be A2 scour-fill clasts, A4 amalgamation clasts and A5 flame-type clasts. Flow-modified clasts include B1 shale clast conglomerates, B2 isolated clasts, B3 clustered clasts, and B5 lamination clasts. This type of environment is characterized by anastomosing flows, channel switching and cannibalization of former beds, so that the most predominant clasts are those formed by erosion, amalgamation and deposition.

Reservoir implications

Deep water massive sands and their associated facies form significant hydrocarbon reservoirs throughout the world. Thick units of more or less structureless sands recovered in core section are not easy to interpret, largely because of their lack of diagnostic features, so that accurate models for further hydrocarbon exploration or production are difficult to construct.

Shale clasts, however, are one of the few diagnostic features that may be present. It therefore becomes important to be able to recognize the type of shale clast or shale clast association present, and hence to infer the probable mode of origin and likely depositional environment within the spectrum of deep water depositional settings that exist. Proximal–distal, marginal–axial channel, lobe or confined basin systems all have a characteristic shale clast signature. Clearly, this must be used in conjunction with all other available data on facies or geometries before a reliable model can be constructed.

Core sections can be used in conjunction with wireline log response (e.g. gamma ray) to gain some idea of probable lateral extent of any particular shale clast horizon. However, used alone, the gamma-ray curves can be misleading as it is not possible to distinguish between muddy sandstones, interbedded sandstones–shales and zones with abundant shale clasts.

Relatively few of the shale clast types described in this study occur with sufficient density and lateral extent to act as significant permeability barriers within reservoir sections. However, it is important to accurately interpret those that may influence vertical permeability in this way, and to distinguish them from those that will simply have local effect.

This work was carried out, in part, during a larger survey of deep-water massive sands, funded by Enterprise, Fina, Oryx, Shell and Texaco. We also thank colleagues and reviewers for their part in helping improve the final manuscript. Barry Fulton drafted the diagrams.

References

Allen, J. R. L. 1982. *Sedimentary Structures: Their character and physical basis. Developments in sedimentology.* Elsevier, Amsterdam.

Anketell, J. M., Ceglia, J. & Dzulynski, S. 1970. On the deformational structures in systems with reversed density gradients. *Annals of the Geological Society of Poland,* **40,** 3–30.

Bagnold, R. A. 1954. Experiments on a gravity-free dispersion of large solid spheres in a Newtonian fluid under shear. *Proceedings of the Royal Society of London, A,* **225,** 49–63.

—— 1956. The flow of cohesionless grains in fluids. *Philosophical Transactions of the Royal Society of London, A,* **249,** 235–297.

Braakenburg, N. E. 1994. *Anatomy of deep water massive sands using examples from Cyprus, Sicily and California,* PhD thesis, University of Southampton.

Branney, M. J. & Kokelaar, B. P. 1992. A reappraisal of ignimbrite emplacement: Progressive aggradation and changes from particulate to non-particulate flow during emplacement of high-grade ignimbrite. *Bulletin of Volcanology,* **54,** 504–520.

Chipping, D. H. 1972. Sedimentary structure and environment of some thick sandstone beds of turbidite type. *Journal of Sedimentary Petrology,* **42,** 587–595.

Chough, S. K. & Chun, S. S. 1988. Intrastratal rip-down clasts, Late Cretaceous Uhangri Formation, southwest Korea. *Journal of Sedimentary Petrology,* **58,** 530–533.

Cremer, M. & Stow, D. A. V. 1986. Sedimentary structures of fine-grained sediments from the Mississippi Fan: thin section analysis. *In:* Bouma, A. H., Coleman, J. M., Meyer, A. W., *et al. Initial reports of the Deep Sea Drilling Project,* **XCVI,** Washington.

Dixon, R. J. *et al.* 1995. Sandstone diapirism and clastic intrusion in the Tertiary fans of the Bruce–Beryl Embayment, Quadrant 9, UKCS. *This volume.*

Finn, W. D. L., Lee, K. W. & Martin, G. R. 1977. An effective stress model for liquefaction. *Journal of Geotechnical, Engineering Division, ASCE,* **103,** 517–533.

Folk, R. L. & Ward, W. 1957. Brazos river bar: a study in the significance of grain size parameters. *Journal of Sedimentary Petrology,* **27,** 3–26.

Johns, D. R., Mutti, E., Rossell, J. & Séguret, M. 1981. Origin of a thick, redeposited carbonate bed in Eocene turbidites of the Hecho Group, south-central Pyrenees, Spain. *Geology,* **9,** 161–164.

Jullien, R. & Meakin, P. 1992. Three dimensional model of particle-size segregation by shaking. *Physical Review Letters,* **69,** 640–643.

Kano, K. & Takeuchi, K. 1989. Origin of mudstone clasts in turbidites of the Miocene Ushikiri Formation, Shimane Peninsula, southwest Japan. *Sedimentary Geology,* **62,** 79–87.

Kleverlaan, K. 1989. Three distinctive feeder-lobe systems within one time slice of the Tortonian Tabernas Fan, SE Spain. *Sedimentology,* **36,** 25–45.

Kneller, B. 1995. Beyond the turbidite paradigm: physical models for deposition of turbidites and their implications for reservoir prediction. *This Volume.*

Kuenen, P. H. H. & Menard, H. W. 1952. Turbidity currents, graded and non-graded deposits. *Journal of Sedimentary Petrology,* **2,** 83–96.

—— & Migliorini, C. 1950. Turbidity currents as a cause of graded bedding. *Journal of Geology,* **58,** 91–127.

Link, M. H., Squires, R. L. & Colburn, I. P. (eds) 1981. *Simi Hills Cretaceous Turbidites Southern California.* Society of Economic Palaeontologists and Mineralogists, Pacific section, Fall Fieldtrip Guidebook.

Lowe, D. R. 1982. Sediment gravity flows II: Depositional models with special reference to the deposits of high density turbidity currents. *Journal of Sedimentary Petrology,* **52,** 279–297.

Mézerais, M. L., Faugères, J. C., Figueiredo, A. G. & Massé, L. 1993. Contour current accumulation off Vema channel mouth, southern Brazil Badin: pattern of a ‘contourite fan”. *In:* Stow, D. A. V. & Faugères, J. C. (eds) *Contourites and Bottom Currents. Sedimentary Geology,* **82,** 173–187.

McKee, E. D. & Goldburg, M. 1969. Experiments of formation of contorted structures in mud. *Bulletin of the Geological Society of America,* **80,** 231–244.

MIDDLETON, G. V. & SOUTHARD, J. B. 1978. Mechanics of sediment movement, *Society of Economic Paleontologists and Mineralogists, Short Course*, **3**, 242.

MUTTI, E. & NILSEN, T. H. 1981. Significance of intraformational rip-up clasts in deep sea fan deposits. *International Association of Sedimentologists, 2nd European Regional Meeting, Bologna, Italy.*

—— & RICCI-LUCCHI, F. 1972. Le torbiditi dell'Appennino settentrionale: introduzione all'analsi di facies. *Memorie della Societa Geologica Italiana*, **11**, 161–199.

PETTIJOHN, F. J., POTTER, P. E. & SIEVER, R. 1973. *Sand and Sandstone.* Springer-Verlag, Berlin.

PICKERING, K. T., HISCOTT, R. N. & HEINS, F. J. 1989. *Deep Marine Environments.* Unwin Hyman, London.

PIPER, D. J. W. & STOW, D. A. V. 1984. The Laurentian Fan-Sohm Abyssal Plain. *Geo-Marine Letters*, **3**, 141–146.

POSTMA, G., NEMEC, W. & KLEINSPEHN, K. L. 1988. Large floating clasts in turbidites: a mechanism for their emplacement. *Sedimentary Geology*, **58**, 47–61.

RUPKE, N. A. 1976. Large Scale slumping in a flysch basin, southwestern Pyrenees. *Journal of the Geological Society, London*, **132**, 121–130.

STAUFFER, P. H. 1967. Grain flow deposits and their implications, Santa Ynez Mountains, California. *Sedimentary Geology*, **37**, 487–508.

SULLWOLD, H. H. 1960. Tarzana Fan, deep submarine fan of late Miocene age Los Angeles County, California. *American Association of Petroleum Geologists Bulletin*, **44**, 433–457.

SURLYK, F. 1987. Slope and deep gully sandstones, Upper Jurassic, East Greenland. *American Association of Petroleum Geologists Bulletin*, **71**, 464–475.

TANAKA, J., MAEJIMA, W., COOMBS, D. S., LANDIS, C. A., HADA, S., YOSHIKURA, S. & SUZUKI, M. 1992. Depositional mechanism of mudclast conglomerates – an example of the Triassic–Jurrassic in the Caples Terrane, New Zealand, *Earth Science*, **46**, 113–120.

WALKER, R. G. 1978. Deep water sandstone facies and ancient submarine fans: models for exploration for stratigraphic traps. *American Association of Petroleum Geologists Bulletin*, **62**, 932–966.

WENTWORTH, C. K. 1922. A scale of grade and class terms for clastic sediments. *Journal of Geology*, **30**, 377–392.